

Effect of Thermal Radiation and Chemical Reaction on Heat and Mass Transfer Flow over a Moving Porous Sheet with Suction and Blowing

Md. Hasanuzzaman¹, and Akio Miyara^{2,3}

1. Graduate School of Science and Engineering, Saga University, Saga-shi, 840-8502, Japan

2. Department of Mechanical Engineering, Saga University, Saga-shi, 840-8502, Japan

3. Kyushu University, International Institute for Carbon-Neutral Energy Research, Fukuoka-shi, 819-0395, Japan

Abstract: In this article, effect of thermal radiation and chemical reaction on heat and mass transfer flow over a moving porous sheet with suction and blowing has been investigated. Thermal radiation and chemical reaction effects are considered. By using appropriate transformations, the governing nonlinear partial equations are transformed into coupled nonlinear ordinary differential equations. Graphs are decorated to explore the influence of physical parameters on the non-dimensional velocity, temperature and concentration distributions. The skin friction, the local Nusselt number and the local Sherwood number are computed and analyzed numerically.

Key words: thermal radiation, chemical reaction, moving sheet, suction and blowing

1. Introduction

Flow of an incompressible viscous fluid and heat transfer phenomena over a stretching sheet have received great attention during the past decades owing to the abundance of practical applications in chemical and manufacturing process, such as polymer extrusion, drawing of copper wires, and continuous casting of metals, wire drawing and glass blowing. The prime aim in almost every extrusion is to maintain the surface quality of the extrudate. The problem of extrusion of thin surface layers needs special attention to gain some knowledge for controlling the coating efficiently. Crane [1] was studied the pioneering work of the flow of Newtonian fluid over a linearly stretching surface. Many researchers [2-8] are extended the pioneering works of Crane [1] to explore various aspects of the flow and heat transfer occurring in an infinite domain

of the fluid surrounding the stretching sheet. After all, these studies treated with a steady flow only. In some cases, the flow field and heat transfer can be unsteady due to a sudden stretching of the flat sheet or by a steep change of the temperature of the sheet.

Hossain et al. [9] explained the effect of radiation on natural convection flow of an optically thick viscous incompressible flow past a heated vertical porous plate with a uniform surface temperature and a uniform rate of suction where radiation is included by assuming the Rosseland discussion approximation. A similarity transformation the flow of a thin liquid film of a power-law fluid by unsteady stretching of a surface which is investigated by Andersson et al. [10]. Later, Andersson et al. [11] analyzed the momentum and heat transfer in a laminar liquid film on a horizontal stretching sheet governed by time-dependent boundary layer equations.

Similarity solutions of the boundary layer equations, which describe the unsteady flow and heat transfer over an unsteady stretching sheet which is presented by

Corresponding author: Md. Hasanuzzaman, Master of Philosophy; research areas/interests: thermal engineering. E-mail: hasan82_kuet@yahoo.com.

Elbashbeshy and Bazid [14]. Thermal radiation plays a very significant role in controlling heat transfer in polymer processing industry. The quality of the final product depends to a great extent on the heat controlling factors, and the knowledge of radiative heat transfer in the system can perhaps lead to a desired product with sought qualities. Dandapat et al. [12] explored how the hydrodynamics and heat transfer in a liquid film on unsteady stretching surface are affected by thermo-capillarity. Tsai et al. [13] studied the non-uniform heat source/sink effect on the flow and heat transfer from an unsteady stretching sheet through a quiescent fluid medium extending to infinity.

In this paper, we investigated the effect of thermal radiation and chemical reaction on heat and mass transfer flow over a moving porous sheet with suction and blowing. Under the consideration of thermal and chemical reaction stratification effects the Mathematical modelling is developed. The effects of various emerging parameters on the velocity, temperature and concentration fields are presented through graphically and tables. The local Nusselt number and the local Sherwood numbers are computed numerically and analyzed.

2. Governing Equations

In this present study on effect of thermal radiation and chemical reaction, we assumed the flow to be laminar flow of a viscous, incompressible fluid past a moving sheet. In order to give way for possible wall fluid suction/injection, the moving sheet is assumed to be permeable. Fig. 1 shows the physical model and the coordinate system.

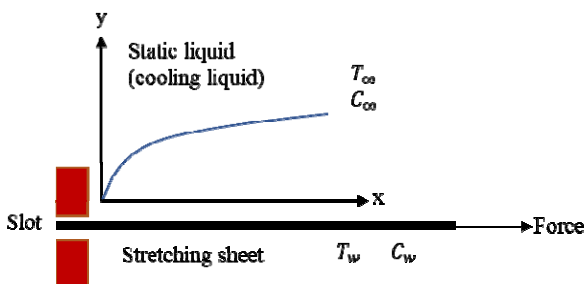


Fig. 1 Physical model and coordinate system.

The governing equations for the continuity equation, momentum equation, energy equation and mass balance equation are given by

$$\frac{\partial u}{\partial x} + \frac{\partial v}{\partial y} = 0 \tag{1}$$

$$u \frac{\partial u}{\partial x} + v \frac{\partial u}{\partial y} = \nu \frac{\partial^2 u}{\partial y^2} - \frac{\mu}{\rho K} u + g\beta_T(T - T_\infty) + g\beta_C(C - C_\infty) \tag{2}$$

$$u \frac{\partial T}{\partial x} + v \frac{\partial T}{\partial y} = \alpha \frac{\partial^2 T}{\partial y^2} + \frac{Q_0}{\rho C_p} (T - T_\infty) + \frac{\beta^* u}{\rho C_p} (T_\infty - T) + \frac{16\sigma^*}{3\rho C_p k^*} T_\infty^3 \frac{\partial^2 T}{\partial y^2} \tag{3}$$

$$u \frac{\partial C}{\partial x} + v \frac{\partial C}{\partial y} = D \frac{\partial^2 C}{\partial y^2} - Kr' C \tag{4}$$

Subject to the following boundary conditions are:

$$u = ax, \quad v = v_w, \quad T = T_w(x) = T_\infty + Ax, \quad C = C_w(x) = C_\infty + Bx \quad \text{at } y = 0 \tag{5}$$

$$u \rightarrow 0, \quad T \rightarrow T_\infty, \quad C \rightarrow C_\infty \quad \text{at } y \rightarrow \infty \tag{6}$$

where u , v , T and C are the velocity, temperature and concentration components in x and y -directions, respectively, g is the acceleration due to gravity, T_w and C_w are as the wall temperature and concentration, respectively, a is the stretching rate which is constant, v_w is the wall suction when ($v_w < 0$) and injection ($v_w > 0$). Also, C_p is the specific heat at constant pressure, ν is the kinematic viscosity, K is the permeability, β_T is the thermal expansion coefficient, β_C is the solutal expansion coefficient, α is the thermal diffusivity of the fluid, D is the mass diffusivity, ρ is the density, $\beta^*(T_\infty - T)$ and $Q_0(T - T_\infty)$ are heat generated or absorbed per unit volume (β^* and Q_0 are constants), σ^* is termed as Stefan-Boltzman constant and k^* is as the mean absorption coefficient and Kr' is the chemical reaction rate of species concentration.

In this paper, we used the relation between the velocity components as well as the stream functions which are given by:

$$u = \frac{\partial \psi(x,y)}{\partial y}, \quad v = -\frac{\partial \psi(x,y)}{\partial x} \tag{7}$$

Also, using the similarity transformations which are given by:

$$\eta = y\sqrt{\frac{a}{\nu}}, \quad \psi = \sqrt{va} xf(\eta), \quad \theta = \frac{T - T_\infty}{T_w - T_\infty},$$

$$\phi = -\frac{c - c_\infty}{c_w - c_\infty} \quad (8)$$

Using the equations (5)-(8), the problems defined in equations (1)-(4) are then transformed into the following set of ordinary differential equations:

$$f''''(\eta) + f(\eta)f''(\eta) - f'^2(\eta) - \frac{1}{Da}f'(\eta) + Gr_T \theta(\eta) + Gr_C \phi(\eta) = 0 \quad (9)$$

$$\theta'(\eta) + \frac{Pr}{1+N_R} [f(\eta)\theta'(\eta) + \Delta\theta(\eta) - \delta_x f'(\eta)\theta(\eta)] = 0 \quad (10)$$

$$\phi''(\eta) + Sc[f(\eta)\phi'(\eta) - Kr_x\phi(\eta)] = 0 \quad (11)$$

with the boundary conditions

$$f(0) = R, \quad f'(0) = 1, \quad \theta(0) = 1, \quad \phi(0) = 1 \quad (12)$$

$$f(\infty) = 0, \quad \theta(\infty) = 0, \quad \phi(\infty) = 0 \quad (13)$$

where primes denote differentiation with respect to η , $R = \frac{v_w}{\sqrt{va}}$ is the dimensionless suction/ blowing velocity, $Da = \frac{aK}{\nu}$ is the Darcy number, $Gr_T = g\beta_T \frac{(T_w - T_\infty)}{a^2x}$ is the Grashof number, $Gr_C = g\beta_C \frac{(c_w - c_\infty)}{a^2x}$ is the modified Grashof number, $Pr = \frac{\nu}{\alpha}$ is the Prandtl number, $N_R = \frac{16\sigma^*T_\infty^3}{3K^*k}$ is the thermal radiation parameter, $\Delta = \frac{Q_0}{\rho C_p a}$ and $\delta_x = \frac{\beta^*x}{\rho C_p}$ are heat generation/absorption coefficients, $Sc = \frac{\nu}{D}$ is the Schmidt number and $Kr_x = \frac{Kr'}{a}$ is the chemical reaction parameter, respectively.

3. Physical Parameters

The physical quantities of interest are the skin friction C_f , the local Nusselt number Nu_x and the local Sherwood number Sh_x which are given by

$$C_f = \frac{1}{2} Re_x^{-\frac{1}{2}} f''(0), \quad Nu_x = Re_x^{\frac{1}{2}} \theta'(0), \quad Sh_x = Re_x^{\frac{1}{2}} \phi'(0) \quad (14)$$

4. Finite Difference Method (FDM)

Our main goal in this article is to apply the finite difference method to solve the problems (9)-(11) with

the boundary conditions (12)-(13). This method has been tested for accuracy and efficiency for solving different problems [16, 17].

By using the transformation $f'(\eta) = z(\eta)$ to convert the system of equations (9)-(11) in the following form:

$$f' - z = 0 \quad (15)$$

$$z'' + fz' - z^2 - \frac{1}{Da}z + Gr_T\theta + Gr_C\phi = 0 \quad (16)$$

$$\theta'' + \frac{Pr}{1+N_R} [f\theta' + \Delta\theta - \delta_x z\theta] = 0 \quad (17)$$

$$\phi'' + Sc[f\phi' - Kr_x\phi] = 0 \quad (18)$$

Subject to the boundary conditions:

$$f(0) = R, z(0) = 1, \theta(0) = 1, \phi(0) = 1 \quad (19)$$

$$f(\infty) = 0, \theta(\infty) = 0, \phi(\infty) = 0 \quad (20)$$

The space of solution's domain is discretized in finite difference methods. By using the following notations: $\Delta\eta = h > 0$ to be the grid size in η -direction, $\Delta\eta = \frac{1}{N}$, with $\eta_i = ih$ for $i = 0, 1, 2, \dots, N$. Define $f_i = f(\eta_i)$, $z_i = z(\eta_i)$, $\theta_i = \theta(\eta_i)$, and $\phi_i = \phi(\eta_i)$. Let F_i, Z_i, θ_i and ϕ_i represent the numerical values of f, z, θ and ϕ at the node i^{th} node, respectively. Then, we get

$$f' \Big|_i \approx \frac{f_{i+1} - f_{i-1}}{2h}, \quad z' \Big|_i \approx \frac{z_{i+1} - z_{i-1}}{2h},$$

$$\theta' \Big|_i \approx \frac{\theta_{i+1} - \theta_{i-1}}{2h}, \quad \phi' \Big|_i \approx \frac{\phi_{i+1} - \phi_{i-1}}{2h} \quad (21)$$

$$z'' \Big|_i \approx \frac{z_{i+1} - 2z_i + z_{i-1}}{h^2},$$

$$\theta'' \Big|_i \approx \frac{\theta_{i+1} - 2\theta_i + \theta_{i-1}}{h^2},$$

$$\phi'' \Big|_i \approx \frac{\phi_{i+1} - 2\phi_i + \phi_{i-1}}{h^2} \quad (22)$$

By using the FDM the main step is that the system of ordinary differential equations (15)-(18) is discretizes in space. Now, using the equations (21)-(22) into the equations (15)-(18) and omitting the truncation errors, finally we get the system of algebraic equations which are given for ($i = 0, 1, 2, \dots, N$):

$$F_{i+1} - F_{i-1} - 2hZ_i = 0 \quad (23)$$

$$Z_{i+1} - 2Z_i + Z_{i-1} + 0.5h[Z_{i+1} - Z_{i-1}] + h^2 \left[Gr_T \theta_i + Gr_C \phi_i - Z_i^2 - \frac{1}{Da} Z_i \right] = 0 \quad (24)$$

$$\theta_{i+1} - 2\theta_i + \theta_{i-1} + \frac{Pr}{1+N_R} 0.5h[F_i(\theta_{i+1} - \theta_{i-1}) + 2h\Delta \theta_i - \delta x Z_i \theta_i] = 0 \quad (25)$$

$$\phi_{i+1} - 2\phi_i + \phi_{i-1} + 0.5h Sc[F_i(\phi_{i+1} - \phi_{i-1}) - 2hKr_x \phi_i] = 0 \quad (26)$$

Also, the boundary conditions are:

$$F_0 = R, Z_0 = 1, \theta_0 = 1, \phi_0 = 1 \quad (27)$$

$$F_N = F_{N-1}, Z_N = Z_{N-1}, \theta_N = \theta_{N-1}, \phi_N = \phi_{N-1} \quad (28)$$

The nonlinear system of algebraic equations are the system of equations (23)-(26) in the variables F_i, Z_i, θ_i and ϕ_i . In our simulations we used the MATLAB package.

5. Results and Discussion

By using the similarity solution technique in MATLAB, the set of ordinary differential equations (9)- (11) with the boundary conditions (12)- (13) are solved numerically. Here the velocity, temperature and concentration are determined as a function of coordinate η . We have adopted a numerical procedure based on MATLAB for getting the solution of the differential equations (9)-(11) with the boundary conditions (12)-(13). The fundamental parameters that governed the flow are the Grashof number, Darcy number, Prandtl number, thermal radiation parameter, heat generation/absorption parameter, Schmidt number and chemical reaction parameter. According to study their effects, a MATLAB programe is written to enumerate and produce the graphs for the velocity, temperature and concentration for different values of these parameters. Few delegate results are given in Figs. 2-9.

Figs. 2(a), (b) and (c) show the effects of the buoyancy force (Grashof number Gr_T) to the viscous forces of a typical velocity, temperature and concentration profiles in the boundary layer,

respectively. From Fig 2(a), it is clear that the momentum boundary layer thickness increases with increasing values of Gr_T enabling more flow. In Fig. 2(b), this figure represents increasing the value of Gr_T outcomes in thinning of thermal boundary layer associated with an increase in the wall temperature gradient and hence produces an increase in the heat transfer rate.

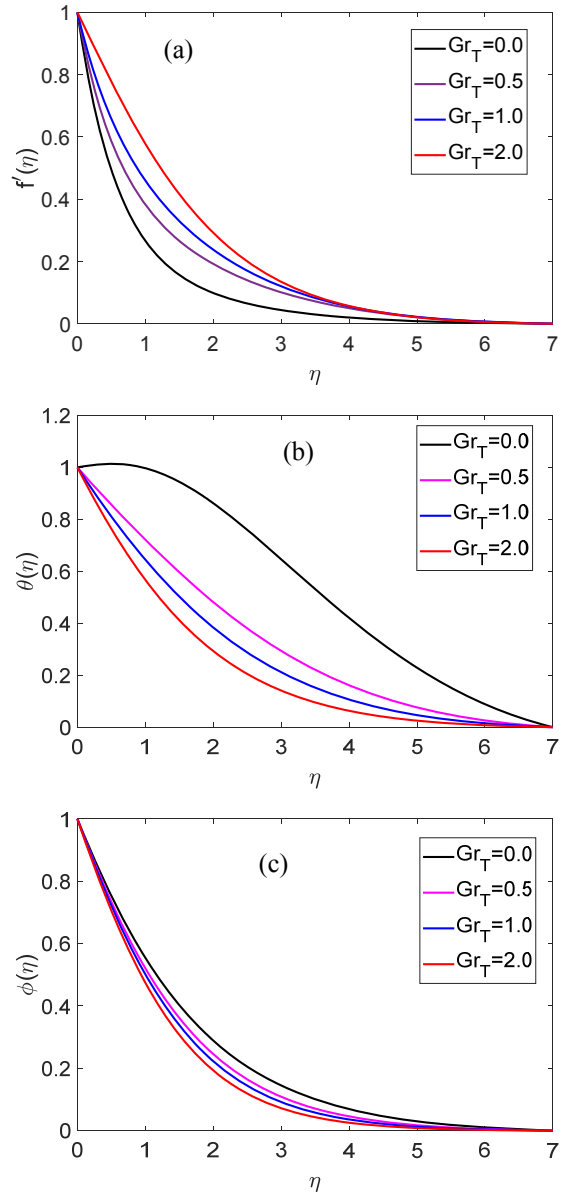


Fig. 2 (a) Velocity, (b) Temperature and (c) Concentration profiles for different values of Grashof number Gr_T with fixed values of $Da = 0.8, R = 0.5, \Delta = 0.5, Pr = 1.0, Sc = 0.5$ and $Kr_x = 0.02$.

It is noticed that the concentration boundary thickness decreases with an increase in the buoyancy force. It is due to fact that an increase in the values of the Grashof number has the tendency to increase the mass buoyancy effect. This gives rise to an increase in the induced flow and there by decrease the concentration which is shown in Fig. 2(c).

The influence of Darcy number on velocity, temperature and concentration profiles are shown in Fig. 3(a), (b) and (c), respectively. From Fig. 3(a), it is observed that the velocity increases with the increase of the Darcy parameter along the sheet and the reverse is true away from the sheet. The dimensionless temperature profiles are displayed in Fig. 3(b).

The influence of suction/blowing parameter R on velocity, temperature and concentration profiles is shown in Figs. 4(a), (b) and (c), respectively. From Fig. 4(a) it is observed that the hydrodynamic boundary layer which shows an increase in the fluid velocity when the imposition of the wall fluid injection increases. However, the exact opposite behavior is produced by imposition of wall fluid suction. From Fig. 4(b), it is observed that with an increase the injection parameters the temperature increases, and the temperature decreases the suction parameter decreases. The same behavior arises for the concentration profiles which is shown in Fig. 4(c).

Figs. 5(a), (b) and (c) represent the effect of heat generation ($\Delta > 0$) or a heat absorption ($\Delta < 0$) in the boundary layer on the velocity, temperature and concentration profiles. From Fig. 5(a), it is observed that increasing the heat generation the fluid velocity increase and for the case of absorption parameter increases the velocity decrease. With an increase the heat generation the temperature increase. This increase in the fluid temperature causes more induced flow towards the plate through the thermal buoyancy effect which shown in Fig. 5(b). From Fig. 5(c) it is clearly observed that increasing the heat generation parameter the concentration decreases and for absorption increasing there is no changed in concentration profile.

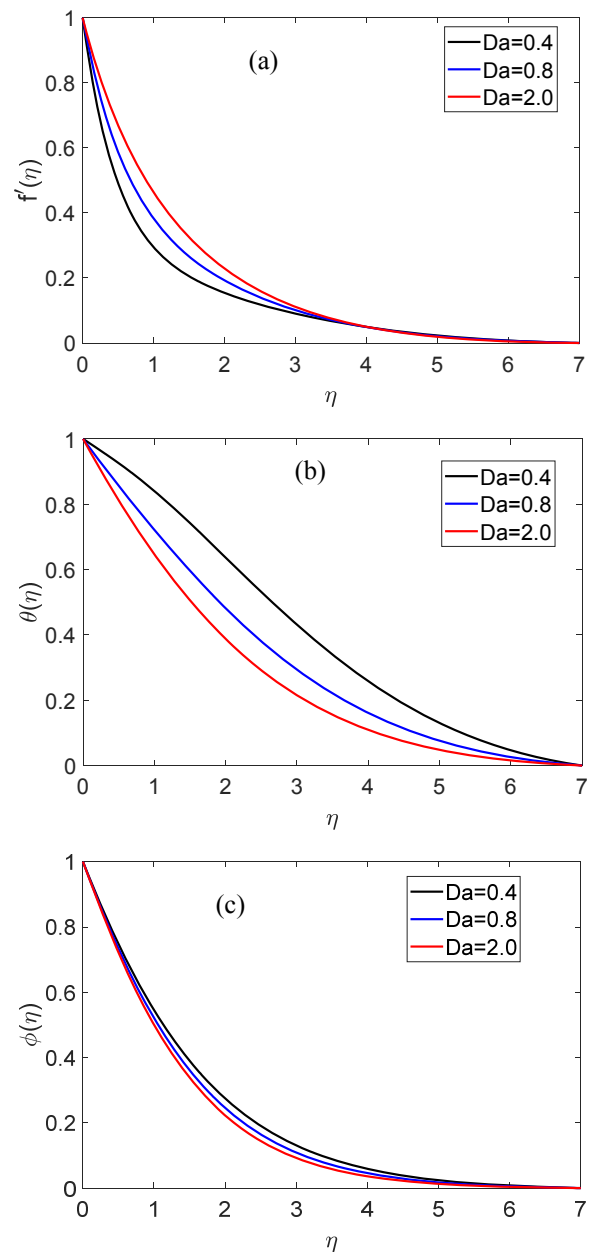


Fig. 3 (a) Velocity, (b) Temperature and (c) Concentration profiles for different values of Darcy number Da with fixed values of $Gr_T = 0.5, R = 0.5, \Delta = 0.5, Pr = 1.0, Sc = 0.5$ and $Kr_x = 0.02$.

Fig. 6 demonstrates the effect of the Prandtl number Pr on the temperature profile. It is observed that with the increase of Prandtl number the temperature decrease. This because a fluid with large Prandtl number possesses large heat capacity, and hence augments the heat transfer.

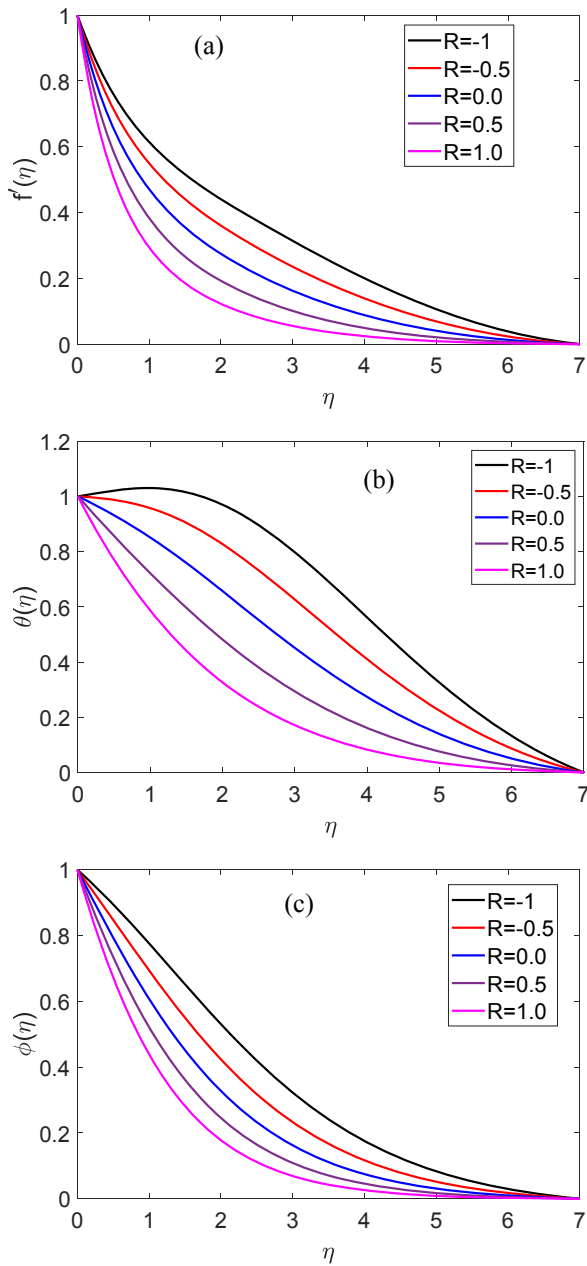


Fig. 4 (a) Velocity, (b) Temperature and (c) Concentration profiles for different values of suction/blowing parameter R with fixed values of $Da = 0.8, Gr_T = 0.5, \Delta = 0.5, Pr = 1.0, Sc = 0.5$ and $Kr_x = 0.02$.

Fig. 7 represents the effect of the radiation parameter N_R on the dimensionless temperature $\theta(\eta)$. It is clearly noticed that the increase of the radiation parameter N_R leads an increase in the temperature at any point. This is due to fact that higher surface heat flux and thereby increasing the temperature of the fluid when the

thermal radiation parameter increases. The variation of the dimensionless concentration against η for different values of the Schmidt number Sc are displayed in Fig. 8. It is clearly observed that with an increase the Schmidt number the concentration decreases. Diffusion coefficient is inversely

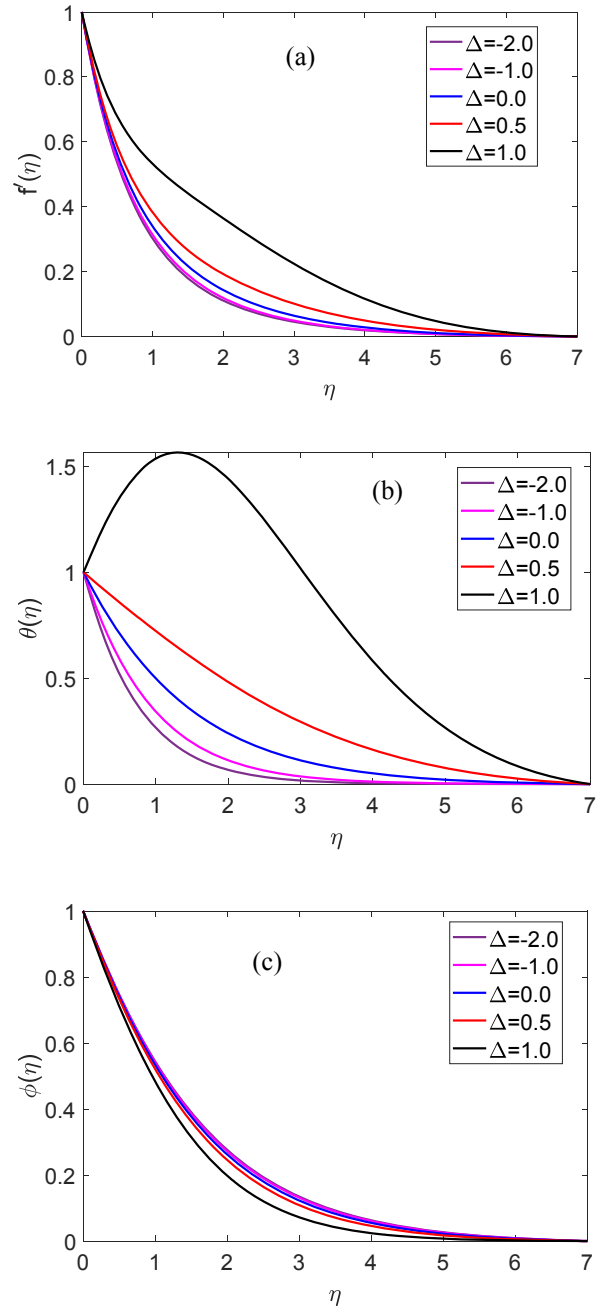


Fig. 5 (a) Velocity, (b) Temperature and (c) Concentration profiles for different values of heat generation/absorption parameter Δ with fixed values of $Da = 0.8, Gr_T = 0.5, R = 0.5, Pr = 1.0, Sc = 0.5$ and $Kr_x = 0.02$.

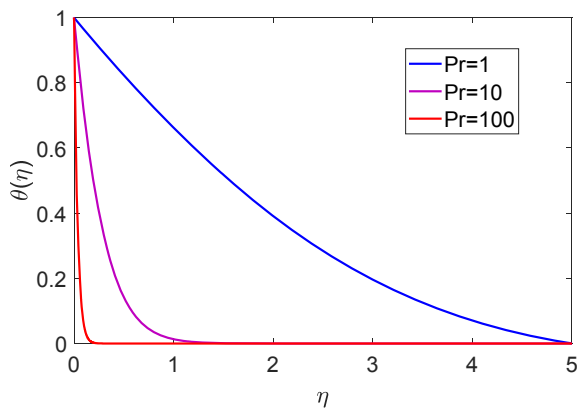


Fig. 6 Temperature profiles for different values of Prandtl number Pr with fixed values of $Da = 0.8$, $Gr_T = 0.5$, $R = 0.5$, $\Delta = 0.5$, $N_R = 1.0$, $Sc = 0.5$, and $Kr_x = 0.02$.

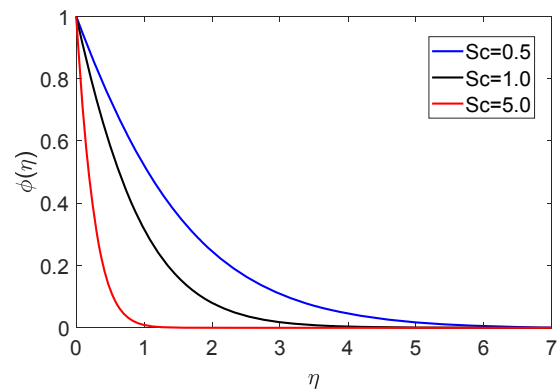


Fig. 8 Concentration profiles for different values of Schmidt number Sc with fixed values of $Da = 0.8$, $Gr_T = 0.5$, $R = 0.5$, $\Delta = 0.5$, $Pr = 1.0$, $N_R = 0.5$, and $Kr_x = 0.02$.

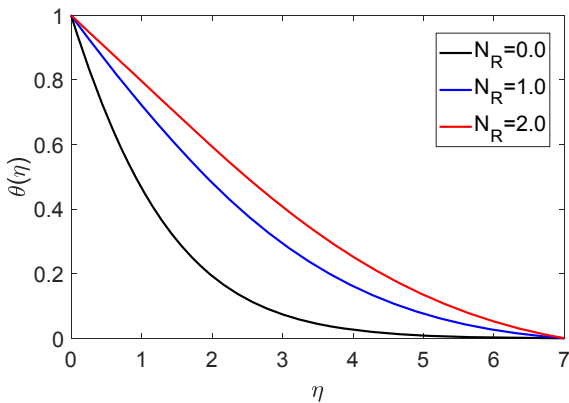


Fig. 7 Temperature profiles for different values of radiation parameter N_R with fixed values of $Da = 0.8$, $Gr_T = 0.5$, $R = 0.5$, $\Delta = 0.5$, $Pr = 1.0$, $Sc = 0.5$, and $Kr_x = 0.02$.

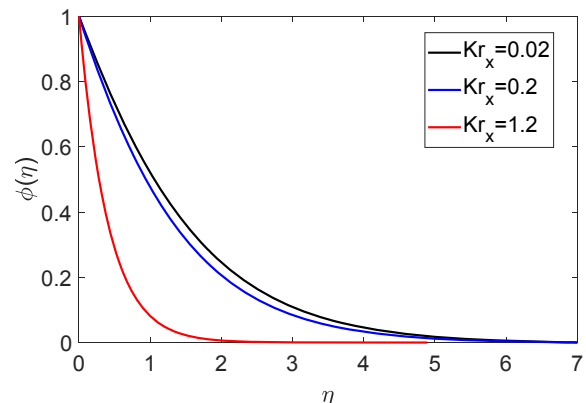


Fig. 9 Concentration profiles for different values of chemical reaction Kr_x with fixed values of $Da = 0.8$, $Gr_T = 0.5$, $R = 0.5$, $\Delta = 0.5$, $Pr = 1.0$, $N_R = 0.5$, and $Sc = 0.5$.

proportional to the Schmidt number. A smaller diffusion coefficient corresponds to an increase in Schmidt number. Such smaller diffusion coefficient creates a reduction in the concentration.

Fig. 9 illustrate the effect of the chemical reaction parameter on the concentration profile. From Fig. 9, it is clearly seen that the concentration and its associated boundary layer thickness are decreasing functions of chemical reaction. Chemical reaction increases the rate of interfacial mass transfer. The concentration gradient and its flux increasing when the chemical reaction reduces the local concentration. Finally, with an increase in the chemical reaction parameter the concentration of the chemical species in the boundary layer decreases.

Fig. 10 illustrates the effect of the Darcy number Da on the skin-friction versus the local Reynolds number. With an increase the Darcy number the skin-friction increase along the local Reynolds number. This is because that a porous media produces a resistive type of force which causes the increase of the skin-friction. Fig. 11 represents the effect of the radiation parameter N_R on the Nusselt number Nu_x along the local Reynolds number Re_x . With an increase the thermal radiation parameter, the Nusselt number Nu_x increases along the local Reynolds number. This is due to fact that for increasing thermal radiation larger heat transfer rates are achieved. Also, with an increase the chemical reaction Kr_x the local Sherwood number Sh_x decrease along the local Reynolds number Re_x . This is

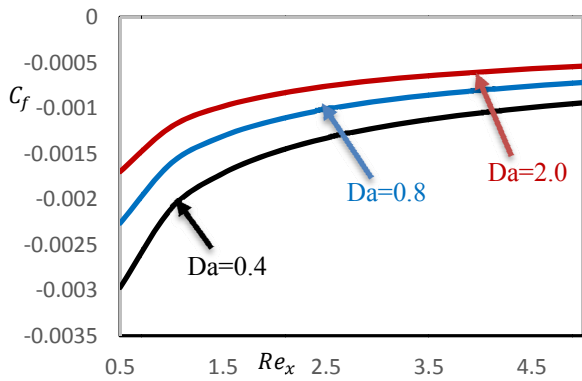


Fig. 10 Variation of Skin-friction C_f with Local Reynolds number Re_x for various Darcy number Da .

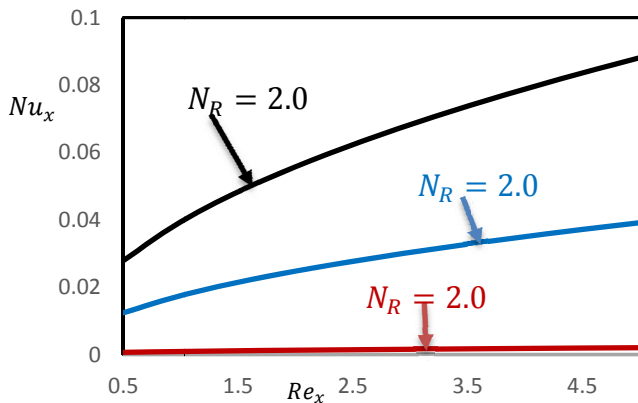


Fig. 11 Variation of local Nusselt number Nu_x with Local Reynolds number Re_x for various thermal radiation parameter N_R .

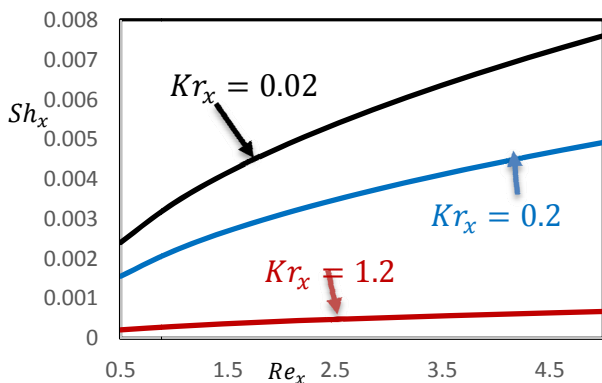


Fig. 12 Variation of local Sherwood number Sh_x with Local Reynolds number Re_x for various thermal radiation parameter Kr_x .

because, for increasing the Chemical reaction parameter smaller mass flow rates are achieved which is shown in Fig. 12.

Table 1 Values proportional to the coefficients of skin-friction ($f''(0)$), rate of heat transfer ($-\theta'(0)$) and the magnitude of the local Sherwood number ($-\phi'(0)$) with the variation of Grashof number Gr_T for fixed $Da = 0.8$, $R = 0.5$, $\Delta = 0.5$, $Pr = 1.0$, $Sc = 0.5$, and $Kr_x = 0.02$.

Gr_T	$f''(0)$	$-\theta'(0)$	$-\phi'(0)$
0.0	-0.0014	-0.0650	-0.0072
0.5	-0.0032	-0.0175	-0.0034
1.0	-0.0029	-0.0096	-0.0022
2.0	-0.0023	-0.0044	-0.0013

Table 2 Values proportional to the coefficients of skin-friction ($f''(0)$), rate of heat transfer ($-\theta'(0)$) and the magnitude of the local Sherwood number ($-\phi'(0)$) with the variation of Darcy parameter Da for fixed, $Gr_T = 0.5$, $R = 0.5$, $\Delta = 0.5$, $Pr = 1.0$, $Sc = 0.5$, and $Kr_x = 0.02$.

Da	$f''(0)$	$-\theta'(0)$	$-\phi'(0)$
0.4	-0.0042	-0.0334	-0.0052
0.8	-0.0032	-0.0175	-0.0034
2.0	-0.0024	-0.0101	-0.0023

Table 3 Values proportional to the coefficients of skin-friction ($f''(0)$), rate of heat transfer ($-\theta'(0)$) and the magnitude of the local Sherwood number ($-\phi'(0)$) with the variation of radiation parameter N_R for fixed $Da = 0.8$, $Gr_T = 0.5$, $R = 0.5$, $\Delta = 0.5$, $Pr = 1.0$, $Sc = 0.5$, and $Kr_x = 0.02$.

N_R	$f''(0)$	$-\theta'(0)$	$-\phi'(0)$
0.0	-0.0012	-0.0009	-0.0052
1.0	-0.0032	-0.0175	-0.0034
2.0	-0.0052	-0.0394	-0.0028

Table 4 Values proportional to the coefficients of skin-friction ($f''(0)$), rate of heat transfer ($-\theta'(0)$) and the magnitude of the local Sherwood number ($-\phi'(0)$) with the variation of Chemical reaction Kr_x for fixed $Da = 0.8$, $Gr_T = 0.5$, $R = 0.5$, $\Delta = 0.5$, $Pr = 1.0$, $N_R = 0.5$, and $Sc = 0.5$.

Kr_x	$f''(0)$	$-\theta'(0)$	$-\phi'(0)$
0.02	-0.0032	-0.0175	-0.0034
0.2	-0.0032	-0.0175	-0.0022
1.2	-0.0032	-0.0175	-0.0003

6. Conclusions

In this present paper, we are tried to investigate the effect of various non-dimensional numbers on the non-dimensional velocity, temperature and concentration fields. The higher values of heat

generation parameter result in higher velocity and temperature distributions and lower concentration distribution. For the higher absorption the velocity and temperature decrease. The concentration gradient and its flux increasing when the chemical reaction reduces the local concentration. Finally, with an increase in the chemical reaction parameter the concentration of the chemical species in the boundary layer decreases. A fluid with large Prandtl number possesses large heat capacity, and hence augments the heat transfer. Moreover, as the thermal radiation increase larger heat transfer rate is achieved as well as the chemical reaction increase smaller mass flow rate is achieved.

References

- [1] L. J. Crane, Flow past a stretching plate, *Zeitschrift fur angewandte Mathematik und Physik* 12 (1970) 645-647.
- [2] M. K. Laha, P. S. Gupta and A. S. Gupta, Heat transfer characteristics of the flow of an incompressible viscous fluid over a stretching sheet, *Warme und Stoffubertrag* 24 (1989) (3) 151-153.
- [3] N. Afzal, Heat transfer from a stretching surface, *International Journal of Heat and Mass Transfer* 36 (1993) (4) 1128-1131.
- [4] K. V. Prasad, A. S. Abel, and P. S. Datti, Diffusion of chemically reactive species of non-Newtonian fluid immersed in a porous medium over a stretching sheet, *The International Journal of Non-Linear Mechanics* 38 (2003) (5) 651-657.
- [5] M. S. Abel and N. Mahesha, Heat transfer in MHD viscoelastic fluid flow over a stretching sheet with variable thermal conductivity, non-uniform heat source and radiation, *Applied Mathematical Modelling* 32 (2008) (10) 1965-1983.
- [6] P. G. Abel, Siddheshwar and M. M. Nandeppanava, Heat transfer in a viscoelastic boundary layer flow over a stretching sheet with viscous dissipation and non-uniform heat source, *International Journal of Heat and Mass Transfer* 50 (2007) (5-6) 960-966.
- [7] R. Cortell, Viscoelastic fluid flow and heat transfer over a stretching sheet under the effects of a nonuniform heat source, viscous dissipation and thermal radiation, *International Journal of Heat and Mass Transfer* 50 (2007) (15-16) 3152-3162.
- [8] C. Wang, Analytic solutions for a liquid film on an unsteady stretching surface, *Heat and Mass Transfer* 42 (2006) 43-48.
- [9] M. A. Hossain, M. A. Alim and D. A. S. Rees, The effect of radiation on free convection from a porous vertical plate, *International Journal of Heat and Mass Transfer* 42 (1999) (1) 181-191.
- [10] H. I. Andersson, J. B. Aarseth, N. Braud and B. S. Dandapat, Flow of a power-law fluid film on an unsteady stretching surface, *Journal of Non-Newtonian Fluid Mechanics* 62 (1996) (1) 1-8.
- [11] H. I. Andersson, J. B. Aarseth and B. S. Dandapat, Heat transfer in a liquid film on unsteady stretching surface, *International Journal of Heat and Mass Transfer* 43 (2000) (1) 69-74.
- [12] B. S. Dandapat, B. Santra, and H. I. Andersson, Thermocapillary in a liquid film on an unsteady stretching surface, *International Journal of Heat and Mass Transfer* 46 (2003) 3009-3015.
- [13] R. Tsai, K. H. Huang and J. S. Huang, Flow and heat transfer over an unsteady stretching surface with non-uniform heat source, *International Communications in Heat and Mass Transfer* 35 (2008) (10) 1340-1343.
- [14] E. M. A. Elbashbeshy and M. A. A. Bazid, Heat transfer over an unsteady stretching surface with internal heat generation, *Applied Mathematics and Computation* 138 (2003) (2-3) 239-245.
- [15] Yahaya Shagaiya Daniel and Simon K. Daniel, Effects of buoyancy and thermal radiation on MHD flow over a stretching porous sheet using homotopy analysis method, *Alexandria Engineering Journal* (2015) (54) 705-712.
- [16] W. T. Cheng and C. H. Liu, Unsteady mass transfer in mixed convective heat flow from a vertical plate embedded in a liquidsaturated porous medium with melting effect, *Int. Commun. Heat Mass Transfer* 35 (2008) 1350-1354.
- [17] A. J. Chamkha, S. A. Ahmed and A. S. Aloraier, Melting and radiation effects on mixed convection from a vertical surface embedded in a non-Newtonian fluid saturated non-Darcy porous medium for aiding and opposing eternal flows, *Int. J. Phys. Sci.* 5 (2010) 1212-1224.
- [18] Md. Hasanuzzaman and Akio Miyara, Similarity solution of natural convective boundary layer flow around a vertical slender body with suction and blowing, *J. Mech. Cont. & Math. Sci.* 11 (2017) 8-22.